Chemical Methodologies 10(2026) 450-464

Chemical Methodologies

Journal homepage: http://chemmethod.com

Original Article

Computational Identification of Natural Product–Based Aryl Hydrocarbon Receptor Modulators for Psoriasis Therapy

Konatham Teja Kumar Reddy[1], G. Surendra[2], E. Joel Mart[3,*], Ramenani Hari Babu[4], Mohamed Shiek Arabath S.A.[5], Phanindra Erukulla[6], Krishna Vamsi Kandimalla[7], Pericharla Venkata Narasimha Raju[8,*]

[1]Department of Pharmaceutical Analysis, Malla Reddy Institute of Pharmaceutical Sciences, Malla Reddy Vishwavidyapeeth (Deemed to be University), Secunderabad, 500100, Telangana, India
[2]School of Pharmacy, ITM University, Turari Campus, Jhansi Road, Gwalior, Madhya Pradesh, India
[3]Department of Pharmacology, Vels Institute of Science, Technology and Advanced Studies (VISTAS), PV Vaithiyalingam Rd, Velan Nagar, Krishnapuram, Pallavaram, Chennai, Tamil Nadu 600117, India
[4]Department of Pharmacy Practice, Teerthanker Mahaveer College of Pharmacy, Teerthanker Mahaveer University, Moradabad 244001, India
[5]Department of Pharmacognosy, Arulmigu Kalasalingam College of Pharmacy, Krishnankoil Tamil Nadu, India
[6]Department of Regulatory Affairs, Ricon Pharma LLC, 100 Ford Rd, Suite 9, Denville, NJ 07834, USA
[7]Department of Regulatory Affairs, InvaGen Pharmaceuticals, A Cipla subsidiary, 550 South Research Place, Central Islip, USA
[8]Department of Regulatory Affairs, Hikma Pharmaceuticals USA, Inc.,2 Esterbrook Lane, Cherry Hill, NJ 08003, USA

ARTICLEINFO

Article history
Submitted: 2025-11-01
Revised: 2025-12-29
Accepted: 2026-01-20
ID: CHEMM-2512-2054

DOI: 10.48309/chemm.2026.563458.2054

KEYWORDS
Psoriasis
AhR
Tapinarof
Pharmacophore screening
Docking
Molecular docking simulation

ABSTRACT

Psoriasis is a chronic inflammatory disease of the skin that needs to be managed in the long term, and the aryl hydrocarbon receptor (AhR) has turned out to be an effective therapeutic target because of its ability to control keratinocyte differentiation and immune signaling. Based on the approved pharmacophore template named Tapinarof, a pharmacophore model was used to screen the ZINC Natural Products Library to identify alternative scaffolds. Three of them, ZINC69482103 (-11.132 kcal/mol), ZINC4098639 (-11.008 kcal/mol), and ZINC13485093 (-10.909 kcal/mol)), more strongly predicted binding to the AhR PAS-B domain than Tapinarof (-10.209 kcal/mol). These molecules also replicate the important aromatic stacking and hydrogen-bond interactions that are significant in the modulation of AhR. The molecular mechanics/generalized Boron surface area (MM-GBSA) analysis also confirmed their high binding potential with ZINC69482103, presenting a favorable ΔG_{bind} value. Simulations of 100 ns using molecular dynamics (MD) ensured the stability of the interaction between the ligands and proteins, remaining at constant values of Root Mean Square Deviation (RMSD), and the contact profile was maintained during the simulation. Drug-likeness and bioavailability assessments with ADMETlab showed that all three compounds were within reasonable physicochemical ranges, with ZINC13485093 exhibiting the most moderate ADMET parameters. In general, the results identified three natural product scaffolds as potential candidates for the development of next-generation AhR modulators for the treatment of psoriasis, particularly ZINC69482103 and ZINC13485093. Their therapeutic potential should be validated through further experiments.

* Corresponding author: E. Joel Mart, Pericharla Venkata Narasimha Raju
E-mail: joelmart5@gmail.com, venkatrapharma@gmail.com

GRAPHICAL ABSTRACT

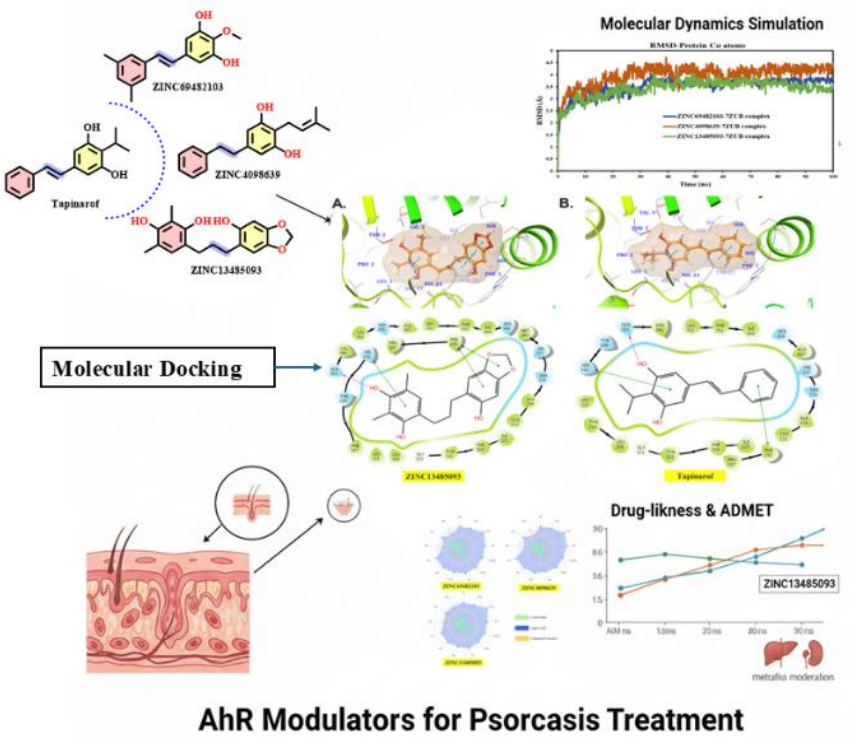

Introduction

Psoriasis is a chronic immune-mediated skin disease characterized by erythematous scaly plaques caused by excessive keratinocyte cell proliferation and inflammation [1-3]. It affects approximately 2–3 percent of the world's population, with significant variation by region. The condition carries a substantial burden, not only due to its visible symptoms, but also because of its association with comorbidities, such as arthritis, metabolic disorders, and decreased quality of life [4,5]. Despite advances in clinical care, psoriasis remains a challenging condition to manage because its pathogenesis involves a complicated combination of genetic predisposition, environmental triggers, and dysregulated immune pathways [6]. The AhR has attracted great interest as a new molecular target for psoriasis. AhR is a ligand-activated transcription factor that is implicated in the sensing of xenobiotics, regulation of immune responses, and skin homeostasis [7]. In psoriatic lesions, AhR signaling is abnormally regulated, which affects cytokine balance, T cell differentiation, oxidative stress, and keratinocyte behavior. Regulation of this receptor restores epidermal integrity and suppresses inflammatory responses [8,9].

Tapinarof is an AhR agonist derived naturally from microbes and has been shown to have a significant therapeutic effect by normalizing epidermal barrier function, suppressing inflammatory cytokines, and reducing oxidative stress [10,11]. AhR stimulation lowers the production of cytokines that play a central role in psoriasis pathogenesis like IL 17A and IL 22, which results in suppressed keratinocyte hyperproliferation and inflammation in psoriatic skin chronic inflammatory signaling [12,13]. These cumulative anti-inflammatory, barrier repairing, and antioxidative effects demonstrate that tapinarof cream 1% has considerable clinical efficacy and remittive effects in plaque psoriasis and that corticosteroid adverse effects are negated [14,15]. Its success further supports the exploration of natural product-based AhR modulators as novel therapeutic agents.

Despite a number of treatment opportunities, including the use of topical agents, phototherapy, systemic immunomodulators, and biologics, the treatment of psoriasis has several complications.

Poor patient adherence, high recurrence rates, concerns about high long-term drug safety, and high costs are factors that lead to suboptimal outcomes. There are also numerous patients with unpredictable responses or tolerance to treatment. These gaps reveals the necessity of safer and more efficacious treatments that can manage upstream controllers of inflammation, including AhR [16-19].

The objective of this work was to determine molecular scaffolds that can bind and activate AhR, having therapeutic effects on psoriasis-related inflammation through the use of computational strategies. For this purpose, the ZINC Natural Products Library, consisting of 142,069 structurally diverse natural compounds, was selected as a screening source. Screening was performed using pharmacophore-based screening with tapinarof as a reference template to acquire the necessary features for AhR activation. The filtered hits were then XP docked and the molecular mechanics/generalized born surface area (MM-GBSA) was scored to rank ligands with good binding affinities. MD was then run to determine the stability of the best complexes and their interaction patterns. Figure 1 depicts the process of selecting and screening a compound.

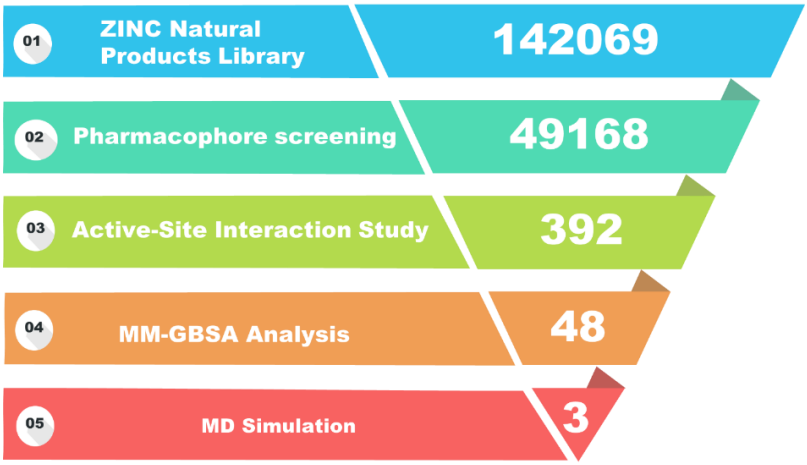

Figure 1: Schematic representation of the step-by-step workflow for screening, docking, and selecting lead compounds targeting the AhR PAS-B domain

Materials and methods

Pharmacophore-Based Virtual Screening

A structure-based pharmacophore model was created with Tapinarof as the reference ligand, considering its reported ability to activate AhR and reduce psoriasis-related inflammation. Key interaction features such as hydrogen bond donors, acceptors, hydrophobic regions, and aromatic sites were identified. This pharmacophore model was used to evaluate the ZINC Natural Products Library. Screening helped to narrow down the molecules that met the essential pharmacophoric requirements for AhR activation. The selection thresholds were defined using Tapinarof as a biological reference rather than arbitrary cut-off values. A pharmacophore fitness score > 2 ensured strong alignment with essential AhR-activating features, whereas docking, and MM-GBSA thresholds were set to retain compounds with binding affinities equal to or better than Tapinarof, thereby prioritizing ligands with a higher likelihood of stable and biologically relevant AhR PAS-B domain interactions.

Ligand and Target Protein Preparation

The ZINC Natural Products Library, which contains 142,069 structurally diverse natural compounds, was prepared using standard ligand preparation protocols such as ionization state generation, stereochemical corrections, and energy minimization [20]. The AhR PAS-B domain (PDB ID: 7ZUB) was downloaded and prepared by inserting missing residues, allocating bond ordering, optimizing hydrogen atoms, and

deleting crystallographic water molecules that are not involved in binding. Prior to docking, the protein structure was refined to eliminate steric conflicts [21]. The prepared ligands were docked into the active site of the AhR PAS-B domain using the XP (extra precision) docking procedure. Docking poses were analyzed using the Glide score, binding orientation, and critical contacts with AhR-activating residues. The top-ranked compounds were selected for further investigation [22,23].

MMGBSA Analysis

To improve the docking data and provide a more precise estimate of ligand affinity, MM-GBSA calculations were conducted on docked ligand–protein complexes. The Prime MM-GBSA technique was used to determine binding free energy (ΔG_{bind}). This approach considers many types of energy, such as molecular mechanics energy, generalized Born solvent accessibility, and terms that rely on the surface area. This method addresses solvation effects and intramolecular strain, which are often not completely taken into account when docking alone. For each complex, the reduced docked posture was reevaluated, and the resultant ΔG_{bind} values were used to rank the compounds. Molecules that demonstrated favorable binding energies, stable interaction patterns, and substantial energetic contributions were selected for further validation using MD simulations [24].

MD Simulation

Desmonds were used to perform MD simulations of docked AhR PAS-B-ligand complexes to investigate their stability and interaction behavior. Each complex was put in an orthorhombic simulation box, solvated with SPC water, neutralized with counterions, and then added 0.15 M NaCl to simulate physiological circumstances [25]. The system was initially energy-minimized to eliminate steric conflicts and then equilibrated via a succession of NVT and NPT processes, with the temperature reaching 300 K and pressure stabilizing at 1 bar [26]. After equilibration, a 100-nanosecond production run was carried out under NPT conditions, with trajectories collected during the simulation [27,28]. Post-run analysis included RMSD to monitor overall structural stability and root mean square fluctuation (RMSF) to measure residue flexibility, hydrogen-bond occupancy, and protein-ligand contact patterns to determine how critical interactions persisted over the simulation. All MD simulations were performed using an HP Z4 workstation with a multi-core Intel CPU, 24GB RAM, and an NVIDIA CUDA-enabled GPU, which provided the computing capability required to conduct long-term simulations efficiently.

Drug-Likeness and Bioavailability Assessment

The drug-likeness and bioavailability profiles of the shortlisted compounds (ZINC69482103, ZINC4098639, and ZINC13485093) were evaluated using *in silico* ADME prediction. The canonical SMILES of each compound were submitted to an online ADMET prediction platform (ADMETlab 3.0) to compute key physicochemical and pharmacokinetic descriptors relevant to oral drug development. The calculated parameters included the molecular weight (MW), lipophilicity indices (logP and logD), aqueous solubility (logS), topological polar surface area (TPSA), number of hydrogen bond donors (nHD) and acceptors (nHA), rotatable bonds (nRot), ring count (nRing), maximum ring size (MaxRing), heteroatom count (nHet), formal charge (fChar), and number of rigid fragments (nRig).

Drug-likeness was assessed by comparing the predicted values against the commonly accepted threshold limits derived from Lipinski's rule of five and related oral bioavailability guidelines. Bioavailability radar plots were generated to visualize the suitability of each compound across six key dimensions: lipophilicity, size, polarity, solubility, flexibility, and saturation. Compounds within the recommended physicochemical range are considered to possess favorable oral drug-like properties. The combined analysis of numerical descriptors and graphical bioavailability radar was used to prioritize compounds with an optimal balance between permeability, solubility, and

structural flexibility for further development as AhR-targeting lead molecules [29-32].

Results and Discussion

Psoriasis is a chronic and often severe immune-mediated skin disorder that affects millions of people worldwide. Its persistent inflammation, high relapse rate, and impact on the quality of life make it a challenging condition to manage. Among the molecular pathways involved, AhR has emerged as a critical regulator of skin homeostasis and inflammatory signaling. Tapinarof is currently the only AhR-targeting drug approved for psoriasis; however, the growing clinical need highlights the urgency to discover new and more effective AhR modulators. To address this gap, a pharmacophore-based virtual screening approach was carried out using tapinarof as the reference template.

Pharmacophore Generation and Hit Identification

The eighth pharmacophore is a key feature of AADDHHRR, which consists of two hydrogen bond acceptors (A), two hydrogen bond donors (D), two hydrophobic features (H), and two aromatic ring centers (R) (Figure 2). These aspects represent the key requirements of the interaction that activates the AhR PAS-B domain. The ZINC Natural Products Library, which consists of 142,069 structurally diverse natural molecules, was screened using a pharmacophore model. The screening resulted in 49,168 hits with a fitness score between 2.683 and -0.3009. Molecules with a score of more than two, totaling 392, were chosen to undergo molecular docking against the AhR PAS-B domain (PDB ID: 7ZUB).

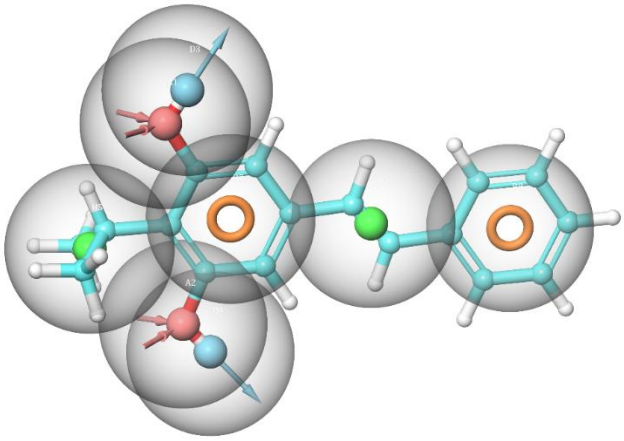

Figure 2: Pharmacophore mapping of the Tapinarof showing the AADDHHRR features

Docking ranged from -13.402 to -3.477 kcal/mol. Both docking and MM-GBSA scores of Tapinarof were used as references to determine the best candidates. Forty-eight compounds showed improved scores compared to Tapinarof in both parameters, indicating improved predicted affinity. Three of them, ZINC69482103, ZINC4098639, and ZINC13485093, not only exhibited full correlation with all AADDHHRR pharmacophore features, but also recapitulated the key binding interactions reported in the Tapinarof-AhR complex (Figures 3 and 4). These molecules are the best hits that can be further evaluated in the future using computational and biological tests.

Docking and Active-Site Interaction Study

Of all the molecules screened, three compounds, namely, ZINC69482103, ZINC4098639, and ZINC13485093, exhibited the best binding affinity to the AhR PAS-B domain, with docking scores almost matching that of the co-crystallized ligand (-13.556 kcal/mol) and better than Tapinarof (-10.209 kcal/mol). The nature of their interaction was also very similar to that of the major residues needed to activate AhR. The three had the highest

affinity with ZINC69482103, having the highest docking score of -11.132 kcal/mol (Table 1). The ligand could bind Phe295, Phe351, and His291 in a strong π–π stacking manner, which stabilized the aromatic scaffolds in the PAS-B pocket. This was supplemented by hydrogen bonding with Gln383, which fixed the ligand at the same site where Tapinarof binds. In general, the pattern of interaction indicated that it was tightly packed in the hydrophobic core and was complementary to the binding cavity (Figure 5A).

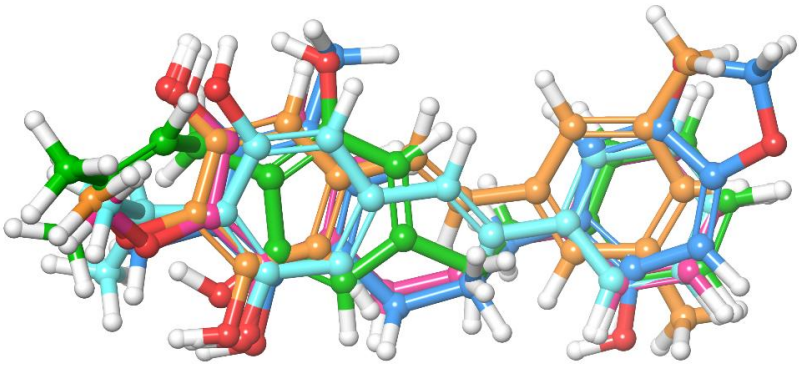

Figure 3: Superimposition of the top-ranked compounds (ZINC69482103, ZINC4098639, and ZINC13485093) onto the reference ligand Tapinarof, showing close spatial alignment

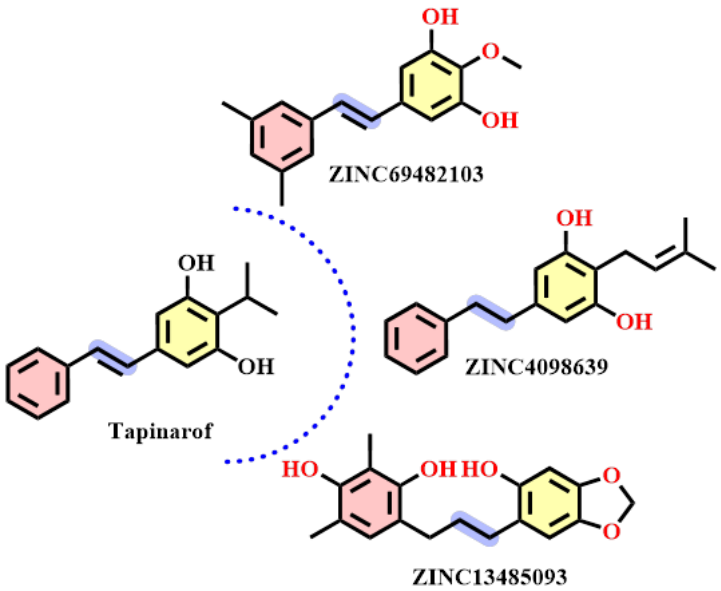

Figure 4: Comparative illustration of structural similarity between the identified lead compounds and Tapinarof, highlighting conserved aromatic and hydrophobic scaffolds essential for AhR PAS-B domain binding

ZINC4098639 had a docking score of -11.008 kcal/mol and retained essential aromatic interactions with Phe295 and His291, similar to tapinarof. It also forms a hydrogen bond with Gln383, which plays a vital role in binding ligands in the pocket. Although the interaction network was slightly smaller than that of ZINC69482103, the high π–π stacking and hydrogen bonding consistency showed a stable and energetically favorable pose (Figure 5B).

Table 1: Summary of pharmacophore fitness, docking scores, and MM-GBSA components for the identified compounds

Title	ZINC69482103	ZINC4098639	ZINC13485093	Tapinarof	Co-crystalized ligand
Fitness	2.63	2.39	2.02	-	-
Docking score	-11.13	-11	-10.9	-10.2	-13.55
ΔG_{bind}	-72.3	-69.46	-65.96	-65.37	-77.81
ΔG_{bind} Coulomb	-9.98	-8.79	-9.17	-11.1	-12.56
ΔG_{bind} H-bond	-0.24	-0.28	-0.24	-0.26	-0.48
ΔG_{bind} Lipo	-48.31	-58.38	-47.66	-48.99	-33.52
ΔG_{bind} Solv GB	26.96	23.88	25.1	25.5	18.38
ΔG_{bind} vdW	-44.06	-32.86	-38.07	-36.45	-47.36

ΔG_{bind}: Overall binding free energy; ΔG_{bind} Coulomb: Electrostatic interaction energy; ΔG_{bind} H-bond: Energy contribution from ligand–protein hydrogen bonds; ΔG_{bind} Lipo: Hydrophobic interaction energy; ΔG_{bind} Solv GB: Solvation penalty based on the Generalized Born model; and ΔG_{bind} vdW: Van der Waals interaction energy reflecting non-polar contacts

ZINC13485093 took second place with -10.909 kcal/mol docking score. This ligand showed a characteristic bidentate aromatic interaction with both Phe295 and His291, which was strongly stabilized by a dual π–π interaction. An additional indication that the ligand was oriented and anchored in the binding region was the presence of a hydrogen bond with Gln383 (Figure 6A). The hydrophobic and aromatic contacts confer high potential for use in AhR modulation. In contrast, Tapinarof generated a docking score of 10.209 kcal/mol and interacted largely with Phe295 and His291 via π–π aromatic stacking and an additional stabilizing hydrogen bond with Gln383 (Figure 6B). These critical interactions were recreated by all three lead compounds with better energetic favorability, indicating their potential as better AhR ligands. Collectively, these results reveal that ZINC69482103, ZINC4098639, and ZINC13485093 not only have better docking scores than Tapinarof, but also have the necessary π–π stacking and hydrogen bonding interactions to allow stable engagement with the AhR PAS-B domain. While docking analysis provided an initial ranking of ligands based on binding orientation and affinity, further refinement was required to account for solvation effects and energetic contributions beyond rigid docking, which was achieved through MM-GBSA binding free energy calculations.

Free Energy Estimation Using MM-GBSA

MM-GBSA calculations were performed to refine the docking results and measure the binding free energy contributions of the top ligands. The ligand that was co-crystallized had the lowest ΔG Bind (-77.81 kcal/mol), which is a robust benchmark for testing newly discovered hits. Of the compounds screened, ZINC69482103 was the best with -72.3 kcal/mol MM-GBSA energy which is close to the co-crystallized ligand and better than Tapinarof (-65.37 kcal/mol). Its high binding energy was prmarily due to large lipophilic contributions (-48.31 kcal/mol) and strong van der Waals interactions (-44.06 kcal/mol) which suggested tight packing in the hydrophobic PAS-B pocket. Its interaction is well explained by the moderate Coulombic term (-9.98 kcal/mol) and the lowest possible contribution of hydrogen bonds.

ZINC4098639 also showed a good overall binding energy of -69.46 kcal/mol with a larger lipophilic preventive energy of -58.38 kcal/mol, indicating a large hydrophobic interaction in the pocket. This compound was a competitive binder; although its van der Waals term (-32.86 kcal/mol) was marginally weaker than that of ZINC69482103,

the overall balance of lipophilic and Coulombic energies placed this compound in a competitive position. Its solvation penalty was also intermediate, indicating good desolvation upon binding.

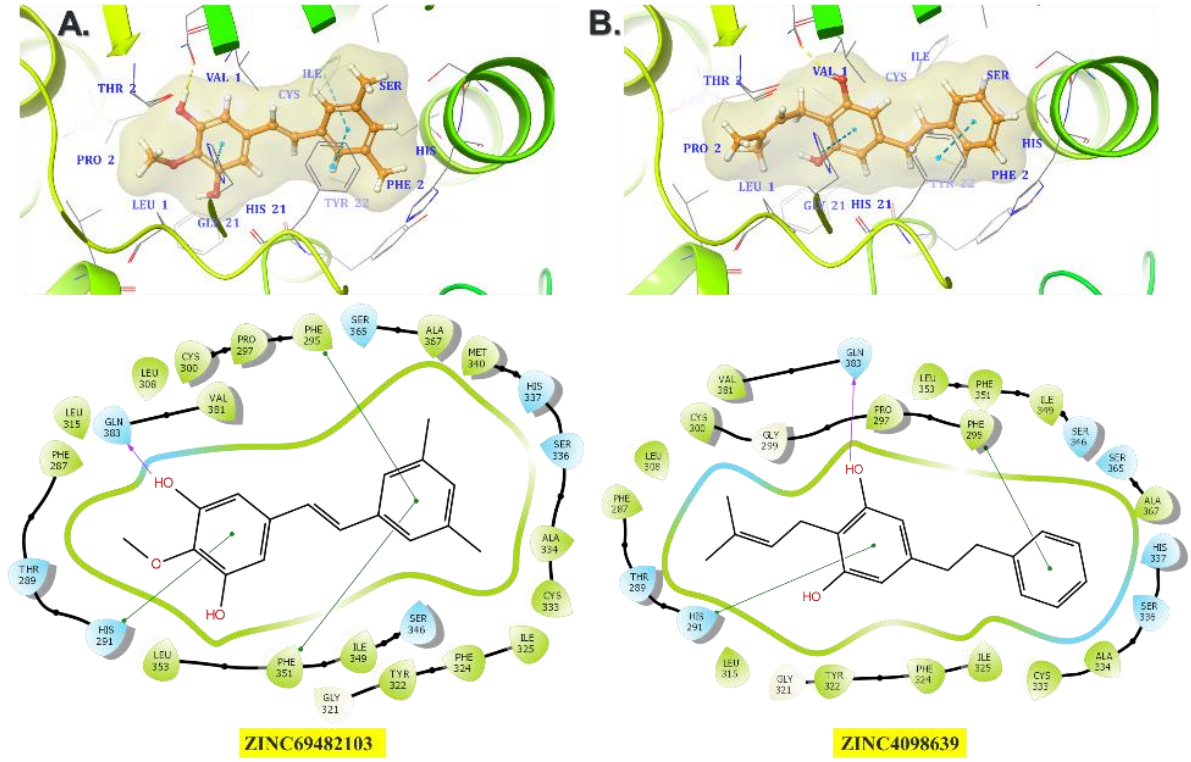

Figure 5: Docking pose and binding interactions of ZINC69482103 (A) and ZINC4098639 (B) in the binding cavity of AhR PAS-B domain (PDB ID: 7ZUB)

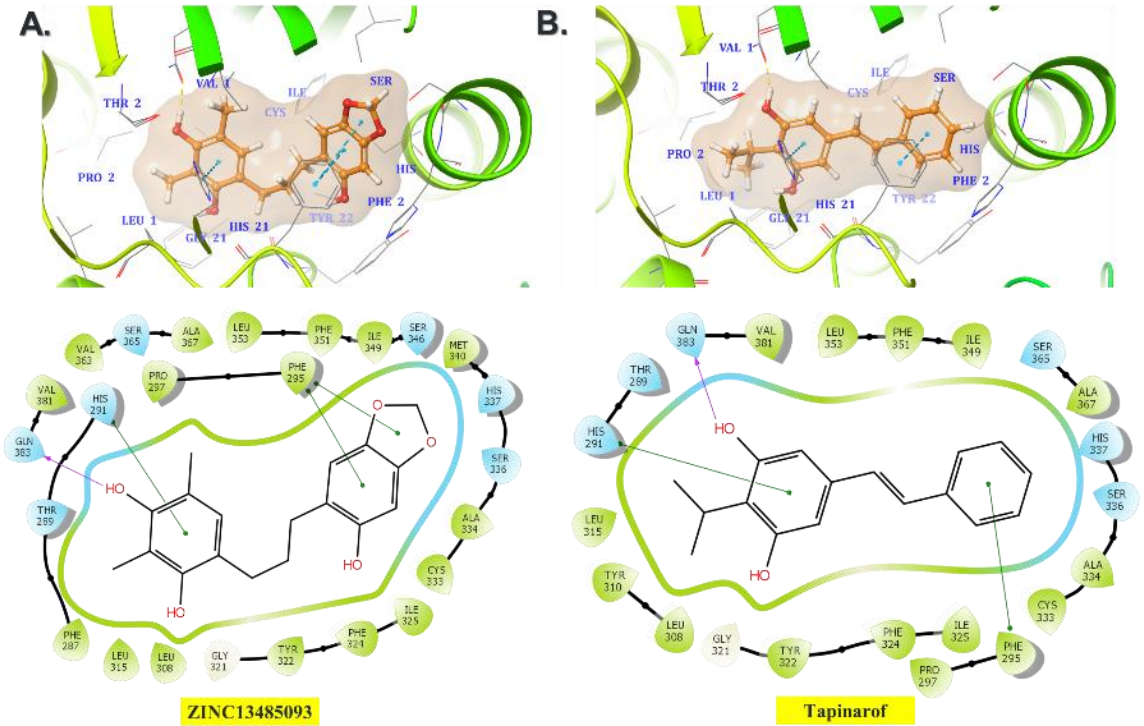

Figure 6: Predicted docking poses of (A) ZINC69482103 and (B) ZINC4098639 in the AhR PAS-B domain (PDB ID: 7ZUB), highlighting key π–π stacking, hydrogen bonding, and hydrophobic interactions with active-site residues

ZINC13485093 showed a binding energy value of -65.96 kcal/mol, which is very similar to that of Tapinarof (-65.37 kcal/mol), but with stronger vdW interactions (-38.07 kcal/mol), which is consistent with its bidentate aromatic interactions with Phe295 and His291. Its affinity is also predicted by its lipophilic term (-47.66 kcal/mol) and constant Coulombic contribution (-9.17 kcal/mol). This equilibrium of energy terms is also in line with the capacity of the ligand to recapitulate the important binding characteristics of Tapinarof. Tapinarof alone had a ΔG_{bind} of -65.37 kcal/mol, with lipophilicity (-48.99 kcal/mol) and vdW contacts (-36.45 kcal/mol) having the greatest influence. Overall, the MM-GBSA results support the docking findings. ZINC69482103 stands out as the best candidate with the highest predicted affinity, followed by ZINC4098639 and ZINC13485093. Their favorable lipophilic and van der Waals contributions imply strong and stable engagement within the hydrophobic core of the AhR PAS-B domain, justifying their selection for further dynamic analysis. Based on the favorable MM-GBSA binding free energy profiles, the top-ranked ligand–AhR PAS-B complexes were selected for MD simulations to evaluate their structural stability and interaction persistence under dynamic physiologically relevant conditions.

MD Simulation for Stability Analysis

To investigate stability and dynamic behavior of the ligand-AhR PAS-B complexes beyond the prediction of the docking results, an MD simulation was carried out. RMSD analysis of the protein Cα atoms throughout the 100 ns trajectory provides insight into the structural stability of the structure as well as the degree of conformational changes when the protein is bound by the ligand. An initial increase in RMSD was observed in all three complexes within the first 10 ns, which is the equilibration phase when the protein changes to adapt to the bound ligand. The trajectories then stabilized and oscillated within reasonable ranges after equilibration, which is a strong indication that all complexes were structurally intact during the simulation.

The structural stability of the three ligand-AhR PAS-B complexes was compared by examining the RMSD profiles of the Ca atoms of the complexes over a 100 ns simulation. There was an initial increase in RMSD in all systems over the first 10 ns, which corresponded to the equilibration phase. Subsequently, both complexes stabilized at a relatively constant plateau, a phenomenon that indicated that the protein-ligand systems were now adapted to the bound conformations.

The ZINC13485093-7ZUB complex was the most stable, with the lowest average RMSD (3.422 Å), maximum RMSD (4.075 Å), and the lowest range of fluctuation (std = 0.37 Å). This indicates that the ligand is compatible with the binding pocket and forms consistent interactions during the simulation (Figure 7). The ZINC69482103-7ZUB complex was also stable with an average standard deviation (0.39 Å) and an RMSD of 3.521 Å. Its stability indicates that the complex is well preserved over time. In contrast, the ZINC4098639-7ZUB complex had slightly more fluctuations, as indicated by the largest average RMSD (3.973 Å), largest maximum RMSD (4.722 Å), and largest standard deviation (0.44 Å). Although this complex generally remains stable, it is structurally more flexible, suggesting that it behaves more dynamically in the binding pocket.

Another statistic, RMSF, was used to study the flexibility of residues in the AhR PAS-B domain durig the 100 ns simulation. RMSF can be used to understand where local motions occur in the protein, as well as to determine whether ligand binding stabilize or perturb a particular residue in the binding pocket.

In all three complexes, the majority of the residues showed low to moderate dynamics, indicating that the general binding region did not alter its structure during simulation. The complex with the lowest average RMSF (1.47 Å) and the least variation spread (std = 0.57 Å) was ZINC13485093-7ZUB, which implies that this ligand causes more rigid and stabilized condition of binding. There was a maximum indication of 11.00 Å but this may be in extreme cases just indicating aspects of flexible loop segments that may have no direct interaction with ligands (Figure 8). The ZINC4098639-7ZUB and

ZINC69482103-7ZUB complexes showed a minor increase in the average fluctuations (1.90 Å each). ZINC69482103 achieved the highest RMSF of 9.69 Å, whereas ZINC4098639 achieved 11.02 Å, meaning that some of the loop's segments are more mobile. However, these motions did not exceed the tolerable limits of the binding pocket and did not affect the stability of the entire binding pocket. Notably, all ligands had stable interactions with the binding residues Thr289, His291, Phe295, Pro297, Cys300, Leu308, Tyr310, Leu315, Ser320, Gly321, Tyr322, Gln323, Phe324, Ile325, Cys333, His337, Met340, Ile349, Phe351, and Leu3, which are associated with the center of the AhR PAS-B domain binding cavity, and their active interaction throughout the trajectory indicates that the process of ligand binding is well preserved throughout the simulation.

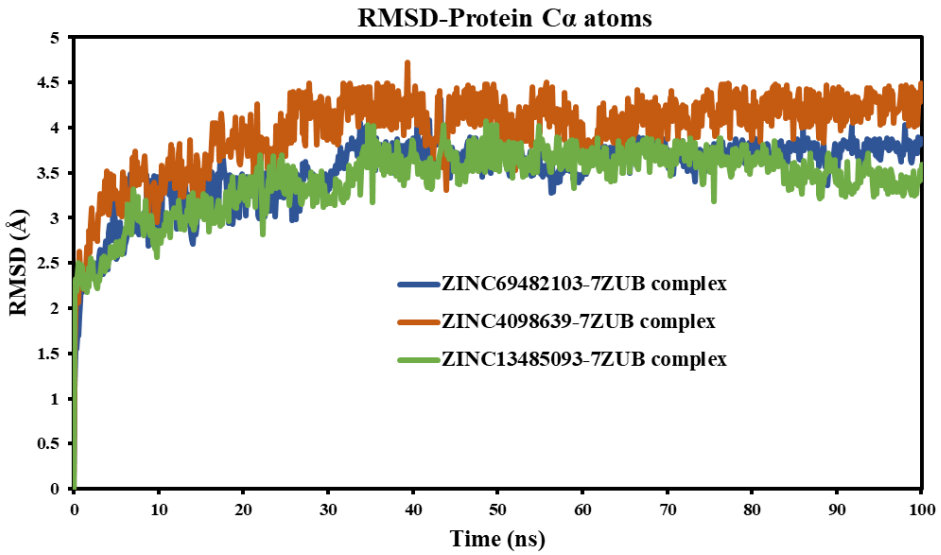

Figure 7: RMSD plot of Cα atoms for the AhR PAS-B domain complexes with ZINC69482103, ZINC4098639, and ZINC13485093 over the 100 ns MD simulation

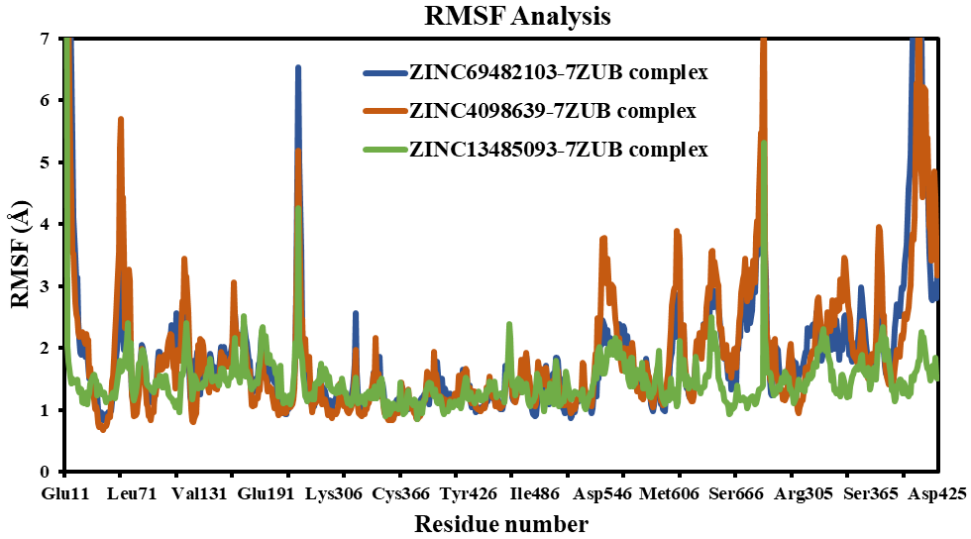

Figure 8: RMSF plot of residue-wise fluctuations in the AhR PAS-B domain during the 100 ns simulation for complexes with ZINC69482103, ZINC4098639, and ZINC13485093

The hydrogen bonding behavior was investigated to determine the level of consistency of each ligand in the binding pocket of the simulated AhR PAS-B. Each of the three complexes could form up to three hydrogen bonds at various locations along the trajectory, meaning that each ligand can be

involved in stabilizing polar interactions under conditions where the protein is in the conformation to allow them to do so. The ZINC4098639-7ZUB complex was the most stable in terms of hydrogen bonds, with an average of 1.79 hydrogen bonds preserved during the entire simulation (Figure 9). This implies that the ligand is still highly bound to the most important polar residues, which helps to maintain its fixed location, even though it exhibits a higher RMSD fluctuation. The ZINC13485093-7ZUB complex was next in line, with an average of 1.73 hydrogen bonds. Although this ligand had the lowest RMSF values and the most stable residue-level environment, it still had a slightly less common hydrogen bonding pattern than ZINC4098639, but a consistent pattern and one supporting stable binding. The ZINC69482103-7ZUB interaction had the lowest number of hydrogen bonds with an average of 1.30. Although this was still high enough to stabilize the ligand, the diminished number of H-bonds indicates that the complex is highly dependent on hydrophobic and π-π interactions, which is also in line with its high docking and MM-GBSA lipophilic contributions. These results indicate that hydrogen bonding significantly contributes to the stability of all three complexes and that ZINC4098639 and ZINC13485093 have the most stable polar interactions, whereas ZINC69482103 has the most stable hydrophobic and aromatic interactions.

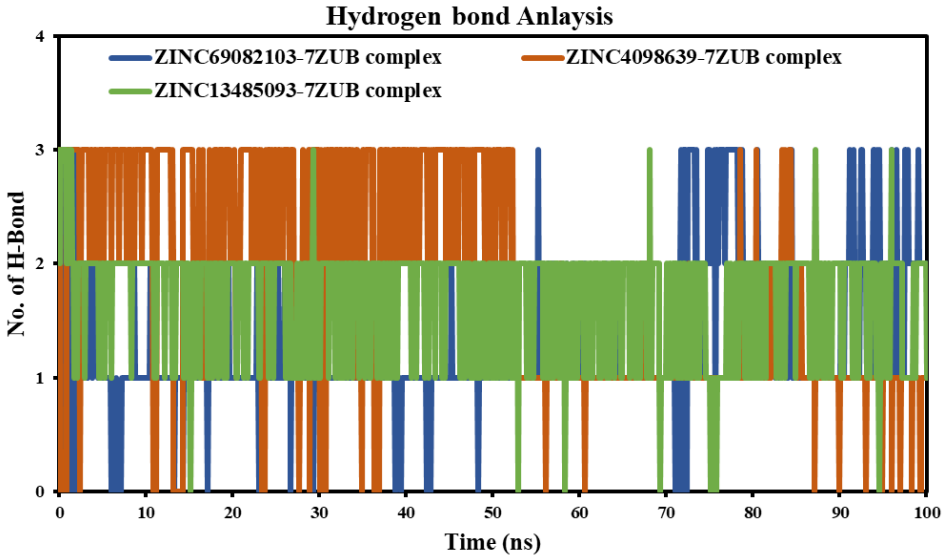

Figure 9: Hydrogen bond occupancy during the 100 ns MD simulation for the AhR PAS-B complexes with ZINC69482103, ZINC4098639, and ZINC13485093

Drug-Likeness and Bioavailability Assessment

The drug-likeness analysis indicated that the three shortlisted compounds were all within the permissible physicochemical space for oral drugs. The bioavailability radar of the identified compounds is shown in Figure 10. The molecular weights fell within the 100-600 Da recommended range, with a span of 270.13 to 316.13, indicating a high level of permeability. The values of TPSA (40.46-79.15 Å^2) are conducive to high membrane diffusion because they are much lower than the maximum value of 140 Å^2. The values for the number of hydrogen bond donors (2-3) and acceptors (2-5) were also within the acceptable range, which also contributed to good passive absorption. ZINC13485093 exhibited the most balanced profile of the three with moderate logP (2.89), acceptable logD (2.78), and highest TPSA (79.15 Å^2), indicating a reasonable compromise between solubility and lipophilicity. ZINC69482103 also had a fairly reasonable profile, albeit with a logP of 4.44, which is slightly higher than the desired upper limit, making it more lipophilic and thus potentially influencing solubility while still promoting high membrane permeability. The logP (5.39) and logD (4.15) values indicated that ZINC4098639 is likely the

most lipophilic of the three and, although this effect could be beneficial in binding to hydrophobic pockets, could lead to challenges in solubility and absorption.

Each of the three compounds was soluble within an acceptable solubility range with logS of -5.08 to -3.32 (Table 2). Although the values for ZINC69482103 and ZINC4098639 were slightly below the desired solubility level (logS > -4), they can still be used with compounds that have strong hydrophobic binding properties. Other descriptors, such as ring count, heteroatom count, rotatable bonds, and rigid fragments, were remained at reasonable numbers to accommodate the satisfactory structural flexibility and conformational stability required for oral drug candidates. Collectively, the parameters of ADME suggest that ZINC13485093 has the most optimal profile in terms of overall drug-likeness and bioavailability, ahead of ZINC69482103. Although ZINC4098639 exhibits good binding properties, its high lipophilicity might necessitate the optimization of the formulation. Generally, all three compounds addressed the most important physicochemical requirements of promising AhR-targeting lead molecules.

Despite the promising outcomes obtained from the integrated computational workflow, the present study had certain limitations. These findings are based exclusively on *in silico* approaches, including molecular docking, MM-GBSA binding free energy calculations, MD simulations, and drug-likeness assessments, which rely on force field approximations and idealized simulation conditions. Although these methods are well-established and widely accepted for early-stage lead identification, they cannot fully capture the complexity of biological systems. Additionally, entropic contributions in the MM-GBSA calculations were approximated, and the predicted drug-likeness and bioavailability parameters represented theoretical estimates rather than experimentally validated pharmacokinetic behavior. Therefore, the predicted binding affinities, stability profiles, and physicochemical suitability of the identified compounds require further experimental validation using *in vitro* AhR activation assays, cellular psoriasis models, and *in vivo* studies to confirm their therapeutic relevance.

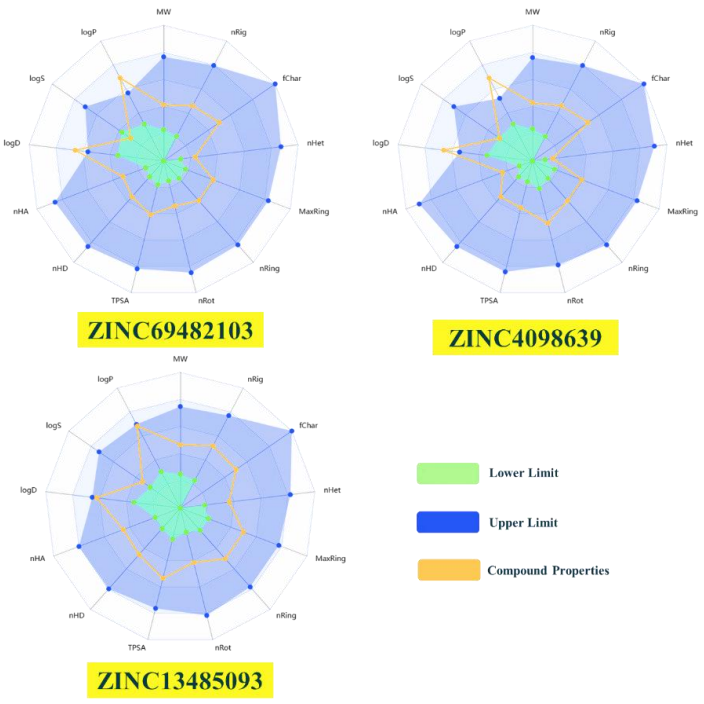

Figure 10: Bioavailability radar illustrating the physicochemical suitability of the shortlisted compounds across key parameters, including lipophilicity, size, polarity, solubility, flexibility, and saturation

Table 2: Physicochemical properties, drug-likeness parameters, and recommended threshold limits for ZINC69482103, ZINC4098639, and ZINC13485093

Parameters	ZINC69482103	ZINC4098639	ZINC13485093	Lower limit	Upper limit
MW	270.13	282.16	316.13	100	600
logP	4.4479	5.3959	2.8958	0	3
logS	-5.0860	-4.0655	-3.3294	-4	0.5
logD	3.8533	4.1563	2.7883	1	3
nHA	3	2	5	0	12
nHD	2	2	3	0	7
TPSA	49.69	40.46	79.15	0	140
nRot	3	5	4	0	11
nRing	2	2	3	0	6
MaxRing	6	6	9	0	18
nHet	3	2	5	1	15
fChar	0	0	0	-4	4
nRig	13	13	16	0	30

Conclusion

In conclusion, this study integrated an *in silico* strategy that combines pharmacophore-based screening, molecular docking, MM-GBSA binding free energy calculations, MD simulations, and ADMET analysis to identify novel natural product–derived AhR modulators. Using Tapinarof as a reference, three lead compounds, ZINC69482103, ZINC4098639, and ZINC13485093, were identified based on favorable pharmacophore alignment, superior docking scores, stable binding free energies, and sustained protein–ligand interactions during 100 ns MD simulations. Among these, ZINC69482103 and ZINC13485093 demonstrated the most promising balance of binding affinity, structural stability, and drug-likeness. Despite these encouraging results, the present study is limited by its purely computational nature. Predicted binding affinities, stability profiles, and pharmacokinetic properties require experimental validation to confirm their biological relevance. Therefore, future work will focus on *in vitro* AhR activation assays, cellular studies in psoriasis-relevant keratinocyte and immune models, and the evaluation of anti-inflammatory efficacy. Additionally, structure–activity relationship optimization and *in vivo* studies will be necessary to further assess therapeutic potential and safety. Overall, this study provides a rational computational foundation for the development of next-generation AhR modulators for psoriasis while clearly outlining the path toward experimental and translational validation.

ORCID

Konatham Teja Kumar Reddy
https://orcid.org/0000-0002-0227-2248
G. Surendra
https://orcid.org/0009-0004-4387-5541
E. Joel Mart
https://orcid.org/0009-0000-9560-674x
Ramenani Hari Babu
https://orcid.org/0009-0006-6396-2110
Mohamed Shiek Arabath S.A.
https://orcid.org/0009-0003-4240-1937
Phanindra Erukulla
https://orcid.org/0009-0001-2900-2881
Krishna Vamsi Kandimalla
https://orcid.org/0009-0004-4526-6045
Pericharla Venkata Narasimha Raju
https://orcid.org/0009-0003-2259-6693

References

[1] Boehncke, W.-H., Schön, M.P. Psoriasis. *The Lancet*, **2015**, 386(9997), 983-994.

[2] Rapp, S.R., Feldman, S.R., Exum, M.L., Fleischer Jr, A.B., Reboussin, D.M. Psoriasis causes as much disability as other major medical diseases. *Journal of the American Academy of Dermatology*, **1999**, 41(3), 401-407.

[3] Soumya, P., Vignanandam, S., Aishwarya, B., Saniya, S., Sofi, S., Kholi, C., Anusha, K. A study to assess the efficacy of various therapeutic strategies used in the treatment of psoriasis. *Journal of Pharmaceutical Sciences and Computational Chemistry*, **2025**, 1(1), 38-49.

[4] Damiani, G., Bragazzi, N.L., Karimkhani Aksut, C., Wu, D., Alicandro, G., McGonagle, D., Wong, P. The global, regional, and national burden of psoriasis: Results and insights from the global burden of disease 2019 study. *Frontiers in Medicine*, **2021**, 8, 743180.

[5] Raharja, A., Mahil, S.K., Barker, J.N. Psoriasis: A brief overview. *Clinical Medicine*, **2021**, 21(3), 170-173.

[6] Feldman, S.R., Goffe, B., Rice, G., Mitchell, M., Kaur, M., Robertson, D., Gottlieb, A. The challenge of managing psoriasis: Unmet medical needs and stakeholder perspectives. *American Health & Drug Benefits*, **2016**, 9(9), 504.

[7] Bissonnette, R., Gold, L.S., Rubenstein, D.S., Tallman, A.M., Armstrong, A. Tapinarof in the treatment of psoriasis: A review of the unique mechanism of action of a novel therapeutic aryl hydrocarbon receptor–modulating agent. *Journal of the American Academy of Dermatology*, **2021**, 84(4), 1059-1067.

[8] Lin, X., Meng, X., Lin, J. The role of aryl hydrocarbon receptor in the pathogenesis and treatment of psoriasis. *Journal of Cutaneous Medicine and Surgery*, **2024**, 28(3), 276-286.

[9] Guo, J., Zhang, H., Lin, W., Lu, L., Su, J., Chen, X. Signaling pathways and targeted therapies for psoriasis. *Signal Transduction and Targeted Therapy*, **2023**, 8(1), 437.

[10] Lin, X., Meng, X., Lin, J. The role of aryl hydrocarbon receptor in the pathogenesis and treatment of psoriasis. *Journal of Cutaneous Medicine and Surgery*, **2024**, 28(3), 276-286.

[11] Silverberg, J.I., Boguniewicz, M., Quintana, F.J., Clark, R.A., Gross, L., Hirano, I., Rubenstein, D.S. Tapinarof validates the aryl hydrocarbon receptor as a therapeutic target: A clinical review. *Journal of Allergy and Clinical Immunology*, **2024**, 154(1), 1-10.

[12] Haarmann-Stemmann, T., Sutter, T.R., Krutmann, J., Esser, C. The mode of action of tapinarof may not only depend on the activation of cutaneous aryl hydrocarbon receptor signaling but also on its antimicrobial activity. *Journal of the American Academy of Dermatology*, **2021**, 85(1), e33-e34.

[13] Jaleel, N., Navya, V., George, M. Tapinarof: A novel topical agent for psoriasis. *Indian Dermatology Online Journal*, **2023**, 14(6), 916-918.

[14] Smith, S.H., Jayawickreme, C., Rickard, D.J., Nicodeme, E., Bui, T., Simmons, C., Mayhew, D. Tapinarof is a natural AhR agonist that resolves skin inflammation in mice and humans. *Journal of Investigative Dermatology*, **2017**, 137(10), 2110-2119.

[15] Eichenfield, L.F., Silverberg, J.I., Hebert, A.A., Chovatiya, R., Brown, P.M., McHale, K.A., Tallman, A.M. Targeting the aryl hydrocarbon receptor to address the challenges of atopic dermatitis. *Journal of Drugs in Dermatology: JDD*, **2024**, 23(2), 23-28.

[16] Armstrong, A.W., Blauvelt, A., Duffin, K.C., Huang, Y.H., Savage, L.J., Guo, L., Merola, J.F. Psoriasis (Primer). *Nature Reviews. Disease Primers*, **2025**, 11(1), 45.

[17] Di Meglio, P., Duarte, J.H., Ahlfors, H., Owens, N.D., Li, Y., Villanova, F., Mrowietz, U. Activation of the aryl hydrocarbon receptor dampens the severity of inflammatory skin conditions. *Immunity*, **2014**, 40(6), 989-1001.

[18] Sá Justo, K., Zonzini Filho, F. Impact of treatment adherence on psoriasis severity: Insights from a multicenter cross-sectional study in Brazil. *Journal of Clinical and Translational Research*, **2025**, 11(4), 64-73.

[19] Yélamos, O., Ros, S., Puig, L. Improving patient outcomes in psoriasis: Strategies to ensure treatment adherence. *Psoriasis: Targets and Therapy*, **2015**, 109-115.

[20] Jadhav, S., Dighe, P. *In vitro* evaluation, and molecular docking studies of novel pyrazoline derivatives as promising bioactive molecules. *Journal of Pharmaceutical Sciences and Computational Chemistry*, **2025**, 1(3), 190-209.

[21] Ban, T., Ohue, M., Akiyama, Y. Multiple grid arrangement improves ligand docking with unknown binding sites: Application to the inverse docking problem. *Computational Biology and Chemistry*, **2018**, 73, 139-146.

[22] Khan, A., Unnisa, A., Sohel, M., Date, M., Panpaliya, N., Saboo, S.G., Khan, S. Investigation of phytoconstituents of Enicostemma littorale as potential glucokinase activators through molecular docking for the treatment of type 2 diabetes mellitus. *In Silico Pharmacology*, **2021**, 10(1), 1.

[23] Khan, S.L., Siddiqui, F.A., Shaikh, M.S., Nema, N.V., Shaikh, A.A. Discovery of potential inhibitors of the receptor-binding domain (RBD) of pandemic disease-causing SARS-CoV-2 Spike Glycoprotein from Triphala through molecular docking. *Current Chinese Chemistry*, **2022**, 2(1), E220321192390.

[24] Dasmahapatra, U., Kumar, C.K., Das, S., Subramanian, P.T., Murali, P., Isaac, A.E., Chanda, K. *In-silico* molecular modelling, MM/GBSA binding free energy and molecular dynamics simulation study of novel pyrido fused imidazo [4, 5-c] quinolines as

potential anti-tumor agents. *Frontiers in Chemistry*, **2022**, 10, 991369.
[25] Alanazi, A., Younas, S., Khan, M.U., Saleem, H., Alruwaili, M., Abdalla, A.E., Ejaz, H. A combined in silico and MD simulation approach to discover novel LpxC inhibitors targeting multiple drug-resistant Pseudomonas aeruginosa. *Scientific Reports*, **2025**, 15(1), 16900.
[26] Joshi, M., Pathan, I., Sahu, A., Raza, A., Sahu, Y., Khatoon, N. Computational Chemistry in Structure-Based Drug Design: Tools, Trends and Transformations, *Journal of Pharmaceutical Sciences and Computational Chemistry*. **2025**, 1(3), 246-266.
[27] Fakola, E.G., Sarkar, A., Uttarkar, A., Bhattacharya, S., Choudhury, S., Ghosh, S., Goswami, P. Integrating the knowledge of traditional medicine to identify potential anti-viral drug against Human Norovirus (HNV); A molecular docking, simulation and network pharmacology analysis. *In Silico Research in Biomedicine*, **2025**, 100090.
[28] Halder, S.K., Sultana, I., Shuvo, M.N., Shil, A., Himel, M.K., Hasan, M.A., Shawan, M.M.A.K. In Silico Identification and Analysis of Potentially Bioactive Antiviral Phytochemicals against SARS-CoV-2: A Molecular Docking and Dynamics Simulation Approach. *BioMed Research International*, **2023**, 2023(1), 5469258.
[29] Xiong, G., Wu, Z., Yi, J., Fu, L., Yang, Z., Hsieh, C., Lu, A. ADMETlab 2.0: an integrated online platform for accurate and comprehensive predictions of ADMET properties. *Nucleic Acids Research*, **2021**, 49(W1), W5-W14.
[30] Siddiqui, F., Bakshi, V. Hydroalcoholic Extraction, Phytoconstituent Profiling by LC-HRMS, and Computational Analysis of Lantana Camara as Potential Glucokinase, Alpha Amylase, Alpha Glucosidase, and DPP-IV Inhibitors, *Chemical Methodologies*. **2025**, 9(12), 1189-1220.
[31] Vikhe, S.R., Patil, S., Ghogare, R., Madkhali, H.A., Khan, M.M.U., Ansari, M.N., Yaidikar, L. Chloroform Extraction, phytochemical screening, GC-HRMS analysis and computational investigation of ehretia laevis Roxb. as potential MELK inhibitor for the treatment of cancer. *Chemical Methodologies*, **2025**, 9(8), 715-736.
[32] Muralidharan, V., Sachdeo, R.A., Singh, L.P., Haque, M., Panigrahy, U., Mishra, A.K., Baig, M.S. Molecular docking and dynamic simulation with admet exploration of natural products atlas compound library to search for potential alpha amylase inhibitors for the t2dm treatment. *Chemical Methodologies*, **2025**, 9, 81-102.

Use your device to scan and read the article online

HOW TO CITE THIS ARTICLE
K.T.K. Reddy, G. Surendra, E.J. Mart, R.H. Babu, M.S. Arabath S.A., P. Erukulla, K.V. Kandimalla, P.V.N. Raju, Computational Identification of Natural Product–Based Aryl Hydrocarbon Receptor Modulators for Psoriasis Therapy. *Chem. Methodol.*, 2026, 10(4) 450-464
DOI: https://doi.org/10.48309/chemm.2026.563458.2054
URL: https://www.chemmethod.com/article_238864.html